Building Technologies & Urban Systems Division
Energy Technologies Area
Lawrence Berkeley National Laboratory

Active multi-mode data analysis to improve fault diagnosis in AHUs

Guanjing Lin[1,2], John House[2], Yimin Chen[2], Jessica Granderson[2]*, Wanpeng Zhang[1]

[1]Tsinghua Shenzhen International Graduate School, Tsinghua University, Shenzhen, Guangdong 518055, China
[2]Building Technology and Urban Systems Division, Lawrence Berkeley National Laboratory, 1 Cyclotron Road, Berkeley, CA 94720, USA

Energy Technologies Area
March 2025

DOI: 10.1016/j.enbuild.2025.115621

This work was supported by the Assistant Secretary for Energy Efficiency and Renewable Energy, Building Technologies Office, of the US Department of Energy under Contract No. DE-AC02-05CH11231.

Active multi-mode data analysis to improve fault diagnosis in AHUs

Guanjing Lin[1,2], John House[2], Yimin Chen[2], Jessica Granderson[2*], Wanpeng Zhang[1]

[1]Tsinghua Shenzhen International Graduate School, Tsinghua University, Shenzhen, Guangdong 518055, China

[2]Building Technology and Urban Systems Division, Lawrence Berkeley National Laboratory, 1 Cyclotron Road, Berkeley, CA 94720, USA

*Corresponding Author: jgranderson@lbl.gov

Abstract

Faults in heating, ventilation and air conditioning systems can lead to increased energy consumption, occupant comfort issues, and reduced equipment lifetime. Commercial fault detection and diagnosis (FDD) tools has been increasingly deployed in U.S. commercial buildings. While they are helping to achieve energy efficiency and operational reliability, there remain gaps in their fault diagnostic capabilities. The diagnostic results often contain multiple distinct candidate root causes (CRCs) or offer no insight into CRCs. This study developed a novel active rule-based multi-mode data analysis method to enhance diagnostic resolution by applying proven rule sets and additional new rules to data from multiple known operational modes. The proposed method was demonstrated using enhanced air handling unit performance assessment rule sets and validated with the simulated data of two air handling units. New metrics, namely, reduced number of CRCs and improvement ratio, were developed to quantify the improvement of fault diagnostic resolution. The validation results showed that the proposed method effectively reduced the number of CRCs in contrast to analyzing data solely for a single mode of operation. It achieved a median improvement ratio of 80% in 19 test cases.

Keywords: Fault diagnosis, air handling unit, multi-mode data analysis, energy management and information system, smart building

1. Introduction

Heating, ventilation, and air conditioning (HVAC) systems constitute a significant portion of energy consumption in commercial buildings. Faults in HVAC systems deteriorate system energy efficiency, indoor environment quality, and may lessen the lifespan of HVAC equipment. A study from the International Energy Agency [1] suggested that re-commissioning existing HVAC systems, particularly in air handling unit (AHU) operations, could potentially save 20–30% of their energy consumption. Hence fault detection and diagnostics (FDD) in building HVAC systems has been a prominent area of research interest for the last three decades [2–4]. Generally, FDD comprises two primary processes: fault detection and fault diagnosis [5]. Fault detection involves identifying fault behaviors within the building, i.e., determining that the operation of the system or equipment is incorrect in some respect. Fault diagnosis focuses on pinpointing the candidate root causes (CRCs) (i.e. physical fault factors in the systems) of these detected faults. In some cases, fault detection and diagnosis are integrated into a single step.

In the past 10–15 years, FDD technology has become one of the fastest growing smart building technologies being implemented in U.S. commercial buildings. There are more than 30 commercial FDD software products available in the U.S. market that are used by facility managers or engineers to improve HVAC system operational performance or used by third-party service providers as a value-add to their customers [6]. While commercial FDD tools are helping to achieve cost-effective energy savings, there remain gaps in their capabilities, particularly in accurate fault diagnosis. According to Frank et al., existing commercial FDD tools provide results using condition-based, behavior-based and outcome-based definitions based upon how the faults are presented [7]. Condition-based faults define the presence of an improper or undesired physical condition in a system or piece of equipment (e.g., stuck valves, return air temperature sensor frozen). Behavior-based faults define improper or undesired behavior during the operation of a system or piece of equipment (e.g., simultaneous heating and cooling and supply air temperature higher than setpoint). Outcome-based faults define the performance (e.g., energy efficiency, energy consumption) deviating from a reference outcome. Crowe et al.’s 2023 fault prevalence study examined the faults reported by FDD tools in multiple years for over 60,000 pieces of HVAC equipment and indicated that behavior-based faults were prominent in the reported faults of commercial FDD tools [8]. Compared with condition-based fault, behavior-based fault presentation has limited diagnostic power, as it reports the observed symptom without pinpointing the specific physical component. The need to improve fault diagnosis capabilities in commercial FDD tools is also reflected in Lin et al.'s 2020 study which evaluated the fault detection and fault diagnosis accuracy of two commercial and one academic FDD tools [9]. For each FDD tool tested, when a behavior-based fault was identified, the provided diagnostic results in some cases included multiple distinct CRCs and in other cases provided no insight into possible reasons for the fault. For example, as shown in Table 1, for the detected behavior-based fault “Supply air temperature higher than setpoint”, the diagnosis results include six CRCs: simultaneous heating and cooling, undersized coils, stuck or broken dampers, stuck or broken valves, broken or uncalibrated sensor, error in control sequences. Given the large volume of faults that routinely arise[8], building facility staff will benefit from FDD tools that minimize the need for further investigation by offering more pinpointed, actionable root cause diagnoses.

Table 1 Example fault detection and diagnosis outputs from FDD offerings [9]

Detection Output	Diagnosis Output
Supply air temperature higher than setpoint	Simultaneous heating and cooling Undersized coils Stuck or broken dampers or valves Broken or uncalibrated sensor Error in control sequences
Possible simultaneous or excess heating and cooling	Valve is not seating properly and is leaking Stuck or broken valve Temperature sensor error or sensor installation error is causing improper control of the valves or other coils
Supply static pressure not tracking setpoint	Fan speed control error Damper malfunction Fan malfunction or failure Uncalibrated or malfunctioning pressure sensor
Leaking heating valve	Leaking heating valve

To inform the development of solutions to improve the fault diagnosis capability in commercial FDD tools, we reviewed the literature pertaining to fault diagnosis in HVAC systems. During the last few decades, several fault diagnosis methods have been studied for building HVAC systems [4,10,3,11]. Zhao et al.'s review [12] classified fault diagnosis methods into data-driven-based or knowledge-driven-based methods. Data-driven-based fault diagnosis methods mainly apply machine learning and statistical techniques to analyze system sensing data. For example, Ebrahimifakhar et al. [13] applied nine well-known classification methods, such as support vector machine, XGBoost, random forests, etc., to isolate rooftop unit faults. These classification methods classify the input data samples to determine whether they are from the normal class or fault class and to further identify which fault class they belong to. A simulated data library of model faults at steady-state operation was used for training and validating the classifications methods, as experimental data is rare and difficult to obtain. The overall accuracy rate ranges from 76.2% to 96.2%. Montazeri and Kargar [14] used simulated data from HVACSIM+ software to train and test principal components analysis (PCA), kernel PCA, and radial basis function neural network methods for AHU fault diagnostics. The results show that the overall accuracy rate using PCA and kernel PCA analysis is 60% and 62%, while faults are detected and diagnosed with 98.7% accuracy when using the neural network approach. Yan et al. [15] utilized generative adversarial network to generate synthetic faulty training data with only a limited set of real-world faulty samples, addressing the challenge of imbalanced training dataset. Other data-driven-based methods investigated include composite neural network [16], k-nearest neighbors [17], deep neural networks [18] and so on. Fueled by advances in artificial intelligence, the number of recent studies about data driven-based diagnosis methods has significantly increased. Recently, large language models (LLMs), a specialized branch of generative artificial intelligence, have shown impressive human-like capabilities in understanding and generating natural language and performing complex problem-solving tasks. The potential of LLMs in fault diagnosis lies in their ability in understanding complex patterns in large datasets from various sources and enabling intuitive, natural language-based communications with users [19]. Zhang et al. [20] developed a fine-tuning method of LLMs supervised by data with fault and fault-free labels to improve the fault diagnosis accuracy of LLMs. In the fine-tuning process, the LLM responses were corrected with misdiagnosed fault classes. The study showed that the fine-tuned generative pre-trained transformers (GPT)-3.5 model increased the fault diagnosis accuracy from 30-40% to nearly 100% in the test cases of an AHU, a variable air volume box, and a chiller plant. Although some data driven-based methods have achieved high accuracy rates, there are several shortcomings to prevent them from being deployed in commercial FDD tools. Firstly, the data driven-based diagnosis methods rely on labeled data of all fault types which is hard to find and collect for real systems. Secondly, they cannot extrapolate beyond the boundaries of training data. And it remains uncertain whether machine learning models trained from an equipment/system can perform well when applied to different ones. Research on utilizing LLMs for building fault diagnosis is still in its early stages. Similar to other data driven-based methods, the main challenge of LLMs lies in the requirements for sufficient labeled fault data. The extremely large number of parameters of LLMs also reduces its interpretability.

Knowledge-driven-based fault diagnosis methods employ physical principles or engineering knowledge and include diagnostic rule-based and inference-based methods. Diagnostic rule-based methods are the norm in commercial FDD tools [21]. An example is fault-tree based method that is based on if-then statements, i.e., if certain conditions are met, then a single or multiple CRCs are provided (Table 1). Bayesian network (BN) is a popular inference-based method that relies on conditional probability theory to predict fault beliefs based on a set of observations. Zhao et al. [22] presented a fault diagnosis method that uses BNs to isolate faults in AHUs. It developed a BN model which describes the probabilistic conditional relations among fault nodes (root causes), evidence nodes (symptoms of faults), and additional information nodes (site investigations, manual tests, maintenance records). The evidence nodes used empirical models of coils, fans, and filters, and these models required training data collected under fault-free operating conditions. The prior probability parameters of the fault nodes in the BN model were estimated by the authors, as there were very few surveys about the frequency of a root cause fault that may happen in AHUs. A BN-based fault diagnosis method was also developed for VAV terminal units [23], chillers [24,25], heat pumps [26], and HVAC systems [27,28]. The main shortcoming of the BN-based method is the need for prior probabilities for all root cause faults. These are normally unknown and values are selected based on experience/engineering knowledge. The literature review above shows that there is still a lack of simple, transparent, and scalable fault diagnosis solutions to be used by commercial FDD tools.

In contrast to previous works, this paper presents a new active rule-based fault diagnosis method to improve root cause isolation and enhance diagnostic resolution by obtaining and combining evidence of both faulty and fault-free behaviors from multiple operational modes. By utilizing data from multiple operating modes, symptoms of a fault that are masked in one mode become evident in another, and evidence of correct operation in one mode can be used to exclude a fault from consideration in another mode. In each case, the effect is to reduce the number of possible condition-based faults that could be producing the observed behavior, thereby improving the diagnosis. The systematic way in which the evidence is combined makes the method extensible to different rule sets and different physical systems, and the simplicity and transparency of the method will help facilitate its adoption by the industry and incorporation into commercial products. The paper demonstrates the effectiveness of the method through two case studies of AHUs.

In summary, this paper provides three novel contributions: (1) A new generalized procedure for combining evidence of both faulty and fault-free behavior from multiple operational modes to facilitate root cause diagnosis. The procedure identifies shared and excluded CRCs by applying proven rule sets and additional new rules to data from multiple known operational modes, and presents the remaining CRCs as the final CRCs. This new method is expected to significantly reduce the number of CRCs in the final diagnosis results, improving the fault diagnostic resolution. (2) Demonstration of the procedure to AHU fault diagnosis using APAR [29,30] - a proven fault detection rule set for assessing AHU operation, and simulation data for two types of AHUs; and refinement of the APAR symptom/fault table and extension of the APAR rule set; and (3) A proposal for new metrics to evaluate the improvement of fault diagnostic resolution.

The remainder of this paper is structured as follows: Section 2 proposes our novel active multi-mode data analysis approach to enhance diagnostic resolution in AHUs. Section 3 presents two case studies using the simulated FDD datasets of an AHU with a heating coil and an AHU without a heating coil, respectively, to demonstrate and evaluate the proposed method, and offers a comparison with the existing single-mode data analysis method. Section 4 presents the discussion. Finally, Section 5 provides the conclusions of the study.

2. Method

HVAC systems operate in various modes such as heating, mechanical cooling, and cooling with outdoor air. These modes change based on external weather conditions and internal building thermal loads. In rule-based fault diagnostic methods used in commercial FDD tools, the HVAC system operational data are collected and analyzed in real time. As a result, only the data from a single operating mode is analyzed, which leads to limited diagnostic insights. The new diagnostic method developed in this paper (Section 2.3) combines the use of multi-operation-mode data from active system testing with proven rule sets and additional auxiliary rules. By complementing the base rule sets with additional engineering logic, and applying them to data from multiple known operational modes, diagnostic resolution can be increased. The new method is described in this section by applying APAR, a well proven AHU FDD rule set, to multi-mode operational data of - single duct variable-air-volume (VAV) or constant-air-volume AHUs; however, the method itself is general and can be extended to other HVAC system types or configurations and other base rule sets. Section 2.1 describes the AHU system configuration and operating sequences. Section 2.2 provides an overview of APAR rule sets. And Section 2.3 illustrates the proposed active multi-mode data analysis method to improve fault diagnosis.

2.1 System description

A schematic diagram showing the components of a typical single duct AHU as well as common measurement and control points is shown in Figure 1.

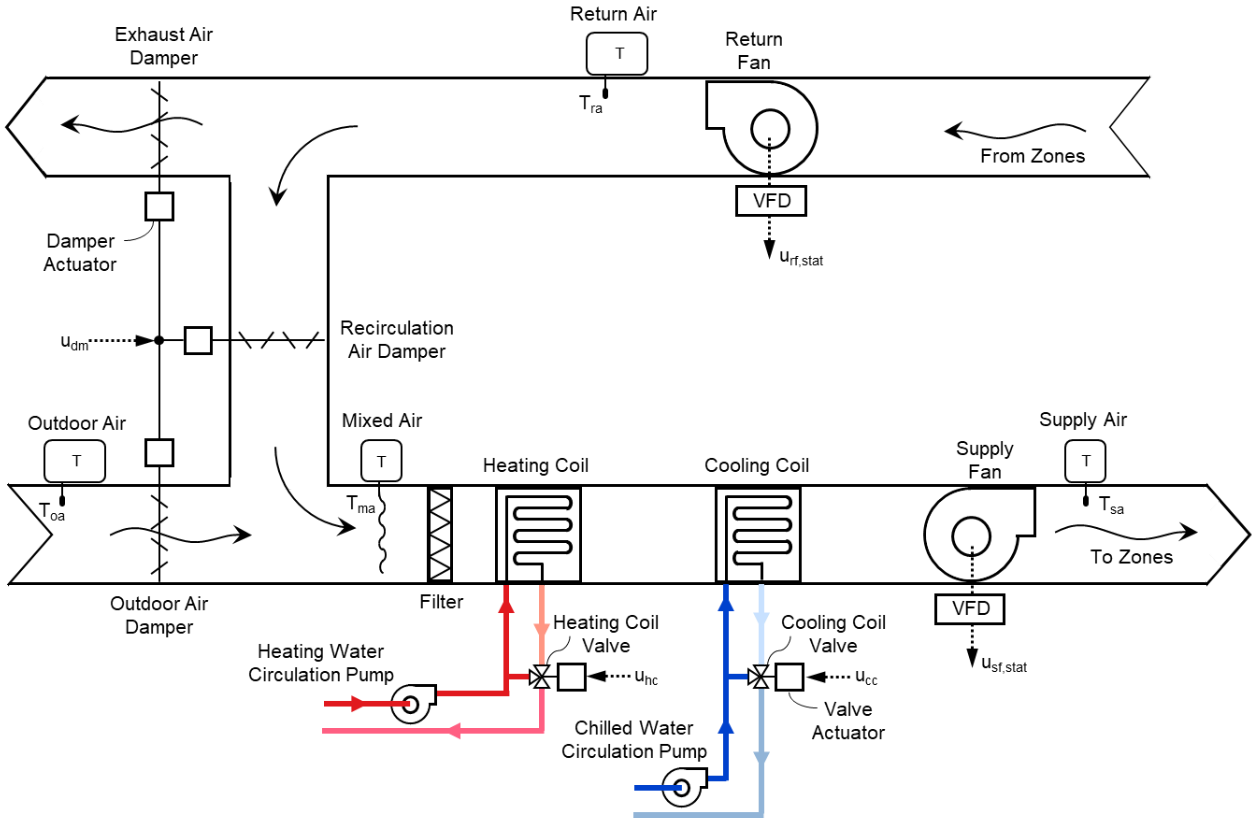

Figure 1 Schematic diagram of a single duct VAV AHU

The typical operating sequence logic for AHUs consists of four primary modes of operation (Figure 2) during occupied hours for maintaining the supply air temperature and ventilation rates at preset levels.

- **Mode 1 (heating)**: the heating coil valve is controlled to maintain the supply air temperature at its setpoint. This mode is normally used in cold outdoor conditions and the outdoor air damper is positioned to enable the minimum amount of outdoor air that will satisfy ventilation requirements. As the outdoor air temperature warms, the heating coil valve will modulate toward the closed position. When the valve is completely closed, the AHU transitions to Mode 2.
- **Mode 2 (cooling with outdoor air)**: the mixing box dampers (outdoor air damper and recirculation damper) modulate and adjust the fraction of outdoor air and return air in the mixed air stream to maintain the supply air temperature at setpoint. As the outdoor air temperature warms, the dampers modulate to allow a higher fraction of outdoor air in the mixed air stream. When the outdoor air damper is fully open, the AHU transitions to Mode 3. If the outdoor air temperature cools, the dampers will modulate to provide a smaller outdoor air fraction.
- **Mode 3 (mechanical cooling with maximum outdoor air)**: the mixing box dampers are controlled for maximum (or 100%) outdoor air and the cooling coil valve is controlled to maintain the supply air temperature at its setpoint. If the outdoor conditions exceed the economizer high limit shutoff, the AHU transitions to Mode 4.
- **Mode 4 (mechanical cooling)**: the mixing box dampers are controlled for minimum outdoor air and the cooling coil valve is controlled to maintain the supply air temperature at setpoint.

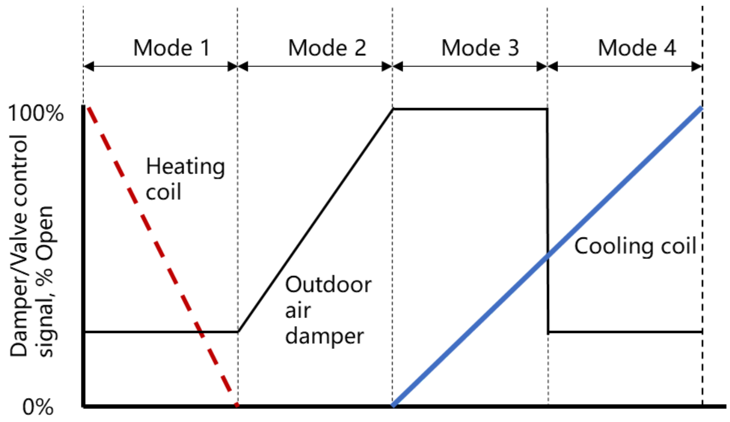

Figure 2 Single-duct AHU operating modes

2.2 Air handling unit performance assessment rules (APAR)

In this section, we introduce APAR, a commonly used rule-based FDD method for single-duct AHUs. It is used to support the description and understanding of the fault diagnostics enhancement approach proposed in this paper (described in Section 2.3). We chose APAR as the proven FDD rules for AHU to demonstrate our generalized procedure because it is widely known in the HVAC FDD community, cited and used in the literature in over 300 publications, and has been implemented in many FDD tools [31, 32, 33].

APAR is a set of expert rules derived from mass and energy balances to detect faults in AHUs [26,27]. Control signals for the heating coil valve, cooling coil valve, and mixing box dampers are used to determine the mode of operation of the AHU in accordance with Eq. (1) - (4). u_{hc} is the normalized heating coil valve control signal [0 - 1] where 0 = closed and 1 = open; u_{cc} is the normalized cooling coil valve control signal [0 - 1] where 0 = closed and 1 = open; u_{dm} is the normalized mixing box damper control signal [0 - 1] where 0 = outdoor air damper at its closed position and 1 = outdoor air damper is 100% open. The tolerances ε_{hc}, ε_{cc} and ε_{dm} are user/developer defined and Mode 5 is an unknown mode of operation for which the control signals are inconsistent with operation in Modes 1-4. APAR consists of 28 rules which are provided in Table 2. Each of the four AHU operating modes has a subset of rules that apply only in that mode. Other rules apply across all four operating modes. The values of the thresholds associated with the rules used in this paper are summarized in Table 3. The setting of thresholds would impact the accuracy of fault detection. Setting the thresholds too low may increase the sensitivity, leading to more false alarms. Setting the thresholds too high can reduce sensitivity, increasing the risk of mis-detection. Among the parameters in Table 3, $(Q_{oa}/Q_{sa})_{min}$ is the design minimum outdoor air fraction. Its value is 0.3 and 0.1 respectively in the two case studies. In the case studies, the other user-defined parameter values were set to the default values provided in House's 2001 APAR study with the exception of ε_{cc}, ε_{dm} and ε_{hc}. These parameters were set to 0.05 instead of the default value of 0.02 to minimize false alarms. When used for other AHU systems, the value of $(Q_{oa}/Q_{sa})_{min}$ should be derived from the control sequence of the test AHU. The settings of other parameters are expected to be appropriate for most circumstances, but it may benefit from tuning the values based on field measurement and operational experience to minimize the false alarms, as excessive false alarms will erode user confidence and responsiveness.

APAR also presents one or more possible candidate root causes (CRCs) for why each of the 28 rules might be triggered, such as a stuck cooling coil valve or a mixed air temperature sensor error. Table 4 tabulates 21 CRCs for the ARAR rules adapted from House's 2001 study [29]. Periodically, a subset of the expert rules applicable to the data from a single operating mode (the current mode of operation) are evaluated to determine if a fault exists. Then the CRCs of the triggered rules are presented as the diagnostics results. This fault diagnosis method is called single-mode data analysis method and used as the reference case for comparison in the case studies.

Mode 1: $u_{hc} > \varepsilon_{hc}$ and $u_{cc} \leq \varepsilon_{cc}$ and $u_{dm} \leq \varepsilon_{dm}$ (1)

Mode 2: $u_{hc} \leq \varepsilon_{hc}$ and $u_{cc} \leq \varepsilon_{cc}$ and $\varepsilon_{dm} < u_{dm} < 1 - \varepsilon_{dm}$ (2)

Mode 3: $u_{hc} \leq \varepsilon_{hc}$ and $u_{cc} > \varepsilon_{cc}$ and $u_{dm} \geq 1 - \varepsilon_{dm}$ (3)

Mode 4: $u_{hc} \leq \varepsilon_{hc}$ and $u_{cc} > \varepsilon_{cc}$ and $u_{dm} \leq \varepsilon_{dm}$ (4)

Mode 5: u_{hc}, u_{cc}, and u_{dm} are inconsistent with Modes 1-4

Table 2 APAR rules from Schein's 2006 study [30]

Mode	**Rule ID**	**Rule Expression (faults are signaled by true expressions)**	**Description**
Mode 1 (Heating with Min OA)	1	$T_{sa} < T_{ma} + \Delta T_{sf} - \varepsilon_t$	T_{sa} is too low relative to T_{ma}.
	2	For $\left\|T_{ra} - T_{oa}\right\| \geq \Delta T_{ra,oa,min}$, $\left\|Q_{oa}/Q_{sa} - (Q_{oa}/Q_{sa})_{min}\right\| > \varepsilon_f$	OA fraction is too low or too high; should equal minimum OA fraction.
	3	$\left\|u_{hc} - 1\right\| \leq \varepsilon_{hc}$ and $T_{sa,set} - T_{sa} \geq \varepsilon_t$	The system is out of control (i.e., the control component is saturated fully open and T_{sa} is unable to meet the setpoint).
	4	$\left\|u_{hc} - 1\right\| \leq \varepsilon_{hc}$	A full heating warning indicating that the system is out of control. If rule 3 is true, rule 4 is suppressed.
Mode 2 (Cooling with Outdoor Air)	5	$T_{oa} > T_{sa,set} - \Delta T_{sf} + \varepsilon_t$	T_{oa} is too high for free cooling without additional mechanical cooling.
	6	$T_{sa} > T_{ra} - \Delta T_{sf} + \varepsilon_t$	T_{sa} is too high relative to T_{ra}.
	7	$\left\|T_{sa} - \Delta T_{sf} - T_{ma}\right\| > \varepsilon_t$	T_{sa} and T_{ma} should be approximately equal.
Mode 3 (Mechanical Cooling with 100%	8	$T_{oa} < T_{sa,set} - \Delta T_{sf} - \varepsilon_t$	T_{oa} is low enough that mechanical cooling is not needed.
	9	$T_{oa} > T_{econ,set} + \varepsilon_t$	T_{oa} is too high for mode 3.

Outdoor Air)	10	$\left\|T_{oa} - T_{ma}\right\| > \varepsilon_t$	T_{oa} and T_{ma} should be approximately equal.
	11	$T_{sa} > T_{ma} + \Delta T_{sf} + \varepsilon_t$	T_{sa} is too high relative to T_{ma}.
	12	$T_{sa} > T_{ra} - \Delta T_{rf} + \varepsilon_t$	T_{sa} is too high relative to T_{ra}.
	13	$\left\|u_{cc} - 1\right\| \leq \varepsilon_{cc}\ and$ $T_{sa} - T_{sa,set} \geq \varepsilon_t$	The system is out of control (i.e., the control component is saturated fully open and T_{sa} is unable to meet the setpoint).
	14	$\left\|u_{cc} - 1\right\| \leq \varepsilon_{cc}$	A full cooling warning indicating that the system is out of control. If rule 13 is true, rule 14 is suppressed.
Mode 4 (Mechanical Cooling with Minimum Outdoor Air)	15	$T_{oa} < T_{econ,set} - \varepsilon_t$	T_{oa} is too low for mechanical cooling with minimum outdoor air.
	16	$T_{sa} > T_{ma} + \Delta T_{sf} + \varepsilon_t$	T_{sa} is too high relative to T_{ma}.
	17	$T_{sa} > T_{ra} - \Delta T_{rf} + \varepsilon_t$	T_{sa} is too high relative to T_{ra}.
	18	For $\left\|T_{ra} - T_{oa}\right\| \geq \Delta T_{ra,oa,min}$, $\left\|Q_{oa}/Q_{sa} - (Q_{oa}/Q_{sa})_{min}\right\| > \varepsilon_f$	OA fraction is too low or too high; should equal minimum OA fraction
	19	$\left\|u_{cc} - 1\right\| \leq \varepsilon_{cc}\ and$ $T_{sa} - T_{sa,set} \geq \varepsilon_t$	The system is out of control (i.e., the control component is saturated fully open and T_{sa} is unable to meet the setpoint).
	20	$\left\|u_{cc} - 1\right\| \leq \varepsilon_{cc}$	A full cooling warning indicating that the system is out of control. If rule 19 is true, rule 20 is suppressed.
Mode 5 (Unknown Mode)	21	$u_{cc} > \varepsilon_{cc}$ and $u_{hc} > \varepsilon_{hc}$ and $\varepsilon_{dm} < u_{dm} < 1 - \varepsilon_{dm}$	Cooling coil valve, heating coil valve and mixing box dampers are modulating simultaneously.
	22	$u_{hc} > \varepsilon_{hc}$ and $u_{cc} > \varepsilon_{cc}$	The cooling coil valve and heating coil valve are modulating simultaneously.
	23	$u_{hc} > \varepsilon_{hc}$ and $u_{dm} > \varepsilon_{dm}$	The heating coil valve and mixing box dampers are modulating simultaneously.
	24	$\varepsilon_{dm} < u_{dm} < 1 - \varepsilon_{dm}$ and $u_{cc} > \varepsilon_{cc}$	The cooling coil valve and mixing box dampers are modulating simultaneously.
All Modes (Modes 1, 2, 3, 4, and 5)	25*	$\left\|T_{sa} - T_{sa,set}\right\| > \varepsilon_t$	$T_{sa,set}$ is not being satisfied
	26	$T_{ma} < \left(T_{ra}, T_{oa}\right) - \varepsilon_t$	T_{ma} is too low; should be between T_{oa} and T_{ra}.
	27	$T_{ma} > \left(T_{ra}, T_{oa}\right) + \varepsilon_t$	T_{ma} is too high; should be between T_{oa} and T_{ra}..
	28	Number of mode transitions per hour > MT_{max}	Too many changes in Operating Mode

*Rule 25 was suppressed whenever rule 3, 13, or 19 is true.

Table 3 User-defined parameter values (e.g., thresholds) used in APAR rules adapted from House's 2001 study [29]

Parameter	Value
MT_{max}	6 transitions
$(Q_{oa}/Q_{sa})_{min}$	0.3 [-]（multiple-zone VAV AHU with heating coil case; 0.1 [-]（multiple-zone VAV AHU without heating coil case
$\Delta T_{ra,oa,min}$	5.5°C
ΔT_{rf}	1.1°C
ΔT_{sf}	1.1° C
ε_{cc}	0.05 [-]
ε_{dm}	0.05 [-]
ε_{f}	0.3 [-]
ε_{hc}	0.05 [-]
ε_{t}	1.6°C

Table 4 Updated table of CRCs for APAR rules from House's 2001 study [29]

APAR Rule ID	Candidate root cause																				
	1-Supply air temperature sensor error	2-Return air temperature sensor error	3-Mixed air temperature sensor error	4-Outdoor air temperature sensor error	5-Leaking cooling coil valve	6-Stuck cooling coil valve	7-Undersized cooling coil	8-Fouled cooling coil	9-Chilled water supply temperature too high	10-Chilled water circulating pump fault	11-Chilled water not available	12-Leaking heating coil valve	13-Stuck heating coil valve	14-Undersized heating coil	15-Fouled heating coil	16-Heating water supply temperature too low	17-Heating water circulating pump fault	18-Leaking mixing box damper(s)	19-Stuck mixing box damper(s)	20-Controller tuning error	21-Controller logic error
1	x		x		x	x							x	x		x	x				
2		x	x	x															x		
3	x				x	x							x	x	x	x	x		x	x	

4	x				x	x							x	x	x	x	x		x	x	
5	x			x	x	x															
6	x	x																			
7	x		x		x	x						x	x								
8	x			x								x	x					x	x		
9																					x
10			x	x														x	x		
11	x		x			x	x		x	x		x	x								
12	x	x				x	x	x	x	x	x	x	x							x	
13	x					x	x	x	x	x	x	x	x							x	
14	x					x	x	x	x	x	x	x	x							x	
15																					x
16	x		x			x	x		x	x		x	x								
17	x	x				x	x	x	x	x	x	x	x							x	
18		x	x	x															x		
19	x					x	x	x	x	x	x	x	x						x	x	
20	x					x	x	x	x	x	x	x	x						x	x	
21																					x
22																					x
23																					x
24																					x
25																				x	
26		x	x	x																	
27		x	x	x																	
28																				x	

Note: The following are updates to the original table in House's 2001 study [29]: **Removed Explanations -** For Rule #2 and Rule #18, leaking mixing box damper(s) is no longer considered a possible explanation for these rules being triggered. Since the dampers are partially open when these rules are evaluated, it is unlikely that leakage would explain any discrepancy between the actual and expected outdoor air fractions. **Added Explanations** - For Rule #3, Rule #4, Rule #19, and Rule #20, stuck mixing box damper(s) is added as a possible explanation. It could result in excessive amounts of very cold or very warm outdoor air entering the AHU, creating loads on the heating and cooling coils that exceed their capacities. As a result, Rule #3 and/or Rule #4 could be triggered in Mode 1, and Rule #19 and/or Rule #20 could be triggered in Mode 4. For Rule #5, stuck or leaking cooling coil valve are added as possible explanations because they could cause Rule #5 to be triggered in Mode 2.

2.3 Active multi-mode data analysis method to improve fault diagnosis

Figure 3 shows the process flow diagram of the proposed active multi-mode data analysis method for enhancing the fault diagnostic resolution of the single-duct AHU. Each step of the process is illustrated in Sections 2.3.1 to 2.3.5. The process is built upon the APAR rule set described in Section 2.2 and extends APAR through the introduction of new rules and the analysis of data from multiple modes of operation. This method is extendable to other HVAC system and equipment.

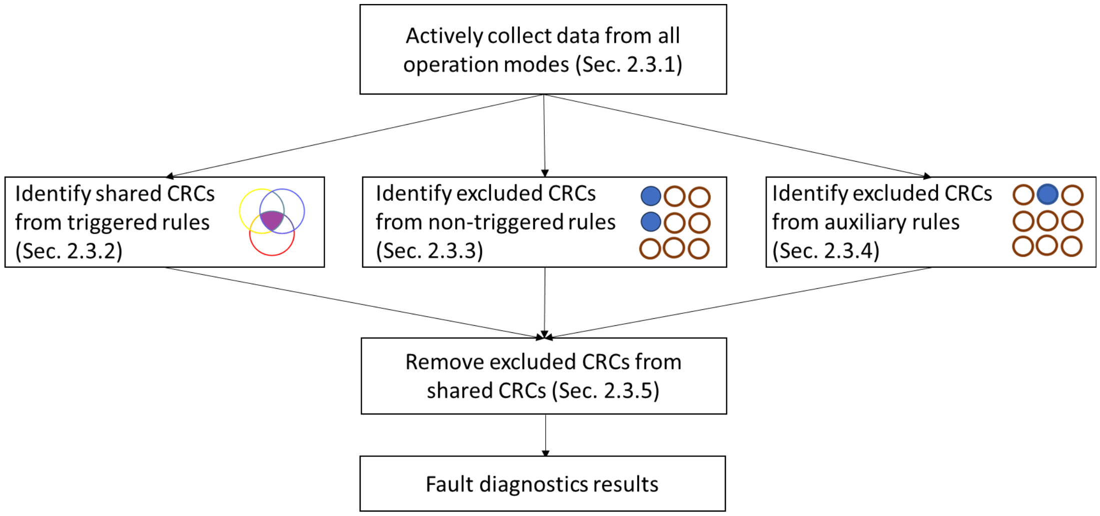

Figure 3 Process flow diagram of multi-mode fault diagnostics method

2.3.1 Collect data from all operating modes

The first step is to conduct proactive tests to cause the AHU sequencing logic to force the unit into each of its normal operating modes. Specifically, change the supply air temperature setpoint ($T_{sa,set}$) and the economizer dry-bulb high limit shutoff setpoint ($T_{econ,set}$) to trigger different operating modes. The values of $T_{sa,set}$ and $T_{econ,set}$ are determined from the values of T_{oa} and T_{ra}. To force operation in Mode 1, $T_{sa,set}$ is set to a value sufficiently greater than the return air temperature. By changing $T_{sa,set}$ to a value between the outdoor and return air temperatures and less than $T_{econ,set}$, the AHU will then transition to Mode 2. Next, $T_{sa,set}$ is changed to a value less than the outdoor air temperature and sufficiently above the chilled water supply temperature, which will force the AHU into Mode 3. Finally, by adjusting $T_{econ,set}$ to a value significantly less than the outdoor air temperature, the AHU will transition to Mode 4. The proactive tests can be performed when 10°C ≤ T_{oa} ≤ T_{ra} − 5.5°C and heating water and chilled water are both available.

- Mode1: $T_{sa,set} = T_{ra} + 2.8°C,\ T_{econ,set} = 23.9°C$
- Mode2: $T_{sa,set} = (T_{oa} + T_{ra})/2,\ T_{econ,set} = 23.9°C$
- Mode3: $T_{sa,set} = \left(T_{oa} - 2.8°C, 10°C\right),\ T_{econ,set} = 23.9°C$
- Mode4: $T_{sa,set} = \left(T_{oa} - 2.8°C, 10°C\right),\ T_{econ,set} = T_{ra} - 5.5°C$

Collect AHU operating data T_{sa}, T_{ra}, T_{oa}, T_{ma}, $T_{sa,set}$, u_{cc}, u_{dm}, u_{hc} and store them at a fixed sampling rate in each operating mode.

2.3.2 Identify shared CRCs from triggered rules

The collected data from all operating modes are divided according to operating mode using Eq. (1) - (4), then the APAR rules (Table 2) are applied to identify if any rules are triggered. If none of the APAR rules are triggered, it is concluded that no fault exists. If one or more of the APAR rules are triggered, there should be a fault. Find the candidate root causes of each triggered rule in Table 4. If there is only one fault present in the AHU, the triggered rules must share at least one condition-based fault among their CRCs. Stated another way, each triggered rule has a set of condition-based faults as CRCs and the intersection of these sets should contain the actual condition-based fault. Therefore, in this step of the process, the knowledge of which APAR rules are triggered is used to find the shared candidate root causes $CRC_{\_share}$ with Eq. (5).

$$CRC_{share} = CRC_1 \cap CRC_2 \cap \ldots \cap CRC_i \quad (5)$$

Where i is the i_{th} rule in Table 4 that is triggered.

2.3.3 Identify excluded CRCs from non-triggered rules

In this step, APAR rules that were *evaluated* and *not triggered* are used to identify CRCs that can be excluded for the detected fault. As we assume that at most there is one root cause present, specific APAR rules that are evaluated and not triggered can be used to remove one or more condition-based faults as possible explanations. Therefore, the knowledge of which APAR rules are not triggered is used to identify excluded faults. Table 5 lists rules that can be used in this way. Also listed for each rule is the condition-based fault that can be removed if the rule is evaluated and not triggered.

For exclusion rule I, if the AHU maintains T_{sa} at $T_{sa,set}$ during the heating mode (Mode 1 - APAR Rule #3 AND Rule #4 are not triggered), it can be concluded that the heating coil valve cannot be stuck and that the heating water circulating pump is operational (i.e., is delivering a sufficient flow of hot water to the heating coil). Thus, stuck heating coil valve and heating water circulating pump fault can be removed as CRCs if APAR Rule #3 AND Rule #4 are evaluated and not triggered. In the same way, exclusion rules IV and V apply to Mode 3 and Mode 4, respectively. For exclusion rule IV, if the AHU maintains T_{sa} at $T_{sa,set}$ during Mode 3 (i.e., APAR Rule #13 and Rule #14 are evaluated and not triggered), it can be concluded that the cooling coil valve is not stuck, the chilled water circulating pump is operational, and chilled water is available. The same faults can be excluded in Mode 4 by exclusion rule V.

For exclusion rule II, when operating in Mode 2, if Rule #7 is evaluated and not triggered, we can conclude that the sensors used in this rule (T_{sa} and T_{ma}) are not faulty and that the heating coil valve and cooling coil valve are not leaking. If any of these faults were present, it would mean that there was one or more additional faults compensating for it and this analysis is built from the assumption that there is at most one fault present at any time. Similarly, for exclusion rule III in Mode 3, if Rule #10 is evaluated and not triggered, we can conclude that the sensors used in this rule (T_{oa}) and (T_{ma}) are not faulty.

Table 5 CRCs that can be removed based on APAR rules that are evaluated in the test and not triggered.

Exclusion rule ID	APAR Rule Evaluated and not Triggered	CRC(s) Removed *
I	#3: $\lvert u_{hc} - 1 \rvert \le \varepsilon_{hc}\ and$ $T_{sa,set} - T_{sa} \ge \varepsilon_t\ and\ u_{hc} > 0$	Stuck heating coil valve *[13]* Heating water circulating pump fault *[17]*

Ⅱ	#7: $\left\|T_{sa} - \Delta T_{sf} - T_{ma}\right\| > \varepsilon_t$	T_{sa} sensor error *[1]* T_{ma} sensor error *[3]* Leaking cooling coil valve *[5]* Leaking heating coil valve *[12]*
Ⅲ	#10: $\left\|T_{oa} - T_{ma}\right\| > \varepsilon_t$	T_{ma} sensor error *[3]* T_{oa} sensor error *[4]*
Ⅳ	#13: $\left\|u_{cc} - 1\right\| \le \varepsilon_{cc}\, and$ $T_{sa} - T_{sa,set} \ge \varepsilon_t\, and\, u_{cc} > 0$	Stuck cooling coil valve *[6]* Chilled water circulating pump fault *[10]* Chilled water not available *[11]*
Ⅴ	#19: $\left\|u_{cc} - 1\right\| \le \varepsilon_{cc}\, and$ $T_{sa} - T_{sa,set} \ge \varepsilon_t\, and\, u_{cc} > 0$	Stuck cooling coil valve *[6]* Chilled water circulating pump fault *[10]* Chilled water not available *[11]*

* The number in italic brackets in the last column corresponds to the explanation number for the CRC from Table 4. For the sake of convenience, these five lines of exclusion rules are referred to by the Roman numerals Ⅰ, Ⅱ, Ⅲ, Ⅳ, Ⅴ in order.

2.3.4 Identify excluded CRCs from auxiliary rules

The idea of removing possible causes or explanations can be extended by adding rules to the existing 28 APAR rules. In this step, we present five auxiliary rules as shown in Table 6. Individual auxiliary rules that are triggered are combined to identify all the CRCs that can be excluded.

Table 6 CRCs that can be removed that can be removed based on auxiliary rules that are evaluated in the test and triggered.

ID	Rule Expression	CRC(s) Removed *
A1	APAR Rule #7 == True and $T_{ma} < T_{sa} - \Delta T_{sf} - \varepsilon_t$ in Mode 2	Leaking cooling coil valve *[5]* Stuck cooling coil valve *[6]*
A2	APAR Rule #7 == True AND $T_{ma} > T_{sa} - \Delta T_{sf} + \varepsilon_t$ in Mode 2	Leaking heating coil valve *[12]* Stuck heating coil valve *[13]*
A3	$\left\|T_{sa} - T_{zda,i}\right\| \le \varepsilon_{zdat}$ for i = 1 to 3 in any Mode	T_{sa} sensor error *[1]*
A4	$\left\|T_{ra} - median(T_{za,i})\right\| \le \varepsilon_{zat}$ for i = 1 to N_z in any Mode	T_{ra} sensor error *[2]*
A5	$\left\|T_{oa} - T_{oa,ws}\right\| \le \varepsilon_{oat}$ in any Mode	T_{oa} sensor error *[4]*

* The number in italic brackets in the last column corresponds to the explanation number for the condition-based fault from Table 4. ε_{zdat} is a user-selected threshold for the zone discharge air temperature. $T_{za,i}$ is the air temperature of zone i, ε_{zat} is a user-selected threshold for the zone air temperature, and N_z is the number of zones considered when determining the median. ε_{oat} is a user-selected threshold for the outdoor air temperature. $T_{oa,ws}$ is the ambient air temperature measured by a local weather station.

The first two auxiliary rules apply in Mode 2 and are derived from APAR Rule #7 (see Table 2). In Mode 2, the heating coil valve and cooling coil valve are commanded closed. Under these conditions, T_{sa} and T_{ma} should differ only by the temperature rise across the fan and any tolerances associated with normal sensor error. Auxiliary Rule #1 indicates that T_{ma} is sufficiently low compared to T_{sa} that there could not be a leaking cooling coil valve fault or a stuck cooling coil valve fault present. Similarly, Auxiliary Rule #2 indicates T_{ma} is sufficiently high compared to T_{sa} that there could not be a leaking heating coil valve fault or a stuck heating valve fault present.

Auxiliary Rule #3 compares T_{sa} to the discharge air temperature (T_{zda}) from several VAV boxes to determine if there is a supply air temperature sensor error. The rule applies in any of the four AHU operating modes, provided the VAV boxes used in the comparison are operating in the cooling or deadband mode (i.e., the valve for the reheat coil must be commanded closed). Auxiliary Rule #3 indicates that if there is agreement between T_{sa} and $T_{zda,i}$ for any of the three VAV boxes used in the comparison, it can be concluded that there is no supply air temperature sensor error. This conclusion holds if Auxiliary Rule #3 is triggered (i.e., satisfied) under any of the four AHU operating modes. Ideally the VAV boxes selected for the comparison should be in close proximity to the AHU. This will help minimize any temperature change due to heat transfer through the supply air ductwork.

Auxiliary Rule #4 compares T_{ra} to the median zone air temperature from a sample of zones served by the AHU. It is recommended that the median be calculated from the temperatures of all zones served by the AHU. If there is agreement between T_{ra} and the median value of the sampled zone temperatures, it can be concluded that there is no return air temperature sensor error. This conclusion holds if Auxiliary Rule #4 is triggered under any of the four AHU operating modes. It should be noted that the threshold ε_{zat} may need to account for a temperature rise across the return fan as well as normal sensor tolerances.

Auxiliary Rule #5 compares T_{oa} to the ambient air temperature measured by a local weather station ($T_{oa,ws}$). Alternatively, for a campus setting, the outdoor air temperature measured at another building could be used. Auxiliary Rule #5 indicates that if there is agreement between T_{oa} and $T_{oa,ws}$, it can be concluded that there is no outdoor air temperature sensor error.

2.3.5. Remove excluded CRCs from shared CRCs

In this step, the procedure removes any CRCs identified in Section 2.3.3 (Identify excluded CRCs from non-triggered APAR rules) and Section 2.3.4 (Identify excluded CRCs from auxiliary rules) from the shared CRCs identified in Section 2.3.2 (Identify shared CRCs from triggered APAR rules). The results after screening are the smallest set of condition-based faults that are identified as the final CRCs.

3. Evaluation case studies

To the best of the authors' knowledge, there are no publicly available experimental datasets that have labeled information on the presence and absence of faults and contain the faulty data with the required ARAR data points across all AHU operational modes. ASHRAE 1312 experimental datasets [34, 35] include a few damper or valve stuck fault cases covering all operation modes, but do not provide damper or valve control signal measurements which are essential in APAR for determining operation mode and triggering rules. Therefore, we used simulated data sets representing the operation of two types of AHUs under faulted conditions to demonstrate the effectiveness of the proposed multi-mode fault diagnostics method. Specifically, we evaluated the new diagnostics method for a multiple-zone VAV AHU with a heating coil and a multiple-zone VAV AHU without a heating coil. For each fault case, the datasets contain the faulty data under all possible operation modes, which means they have the same characteristics with the data obtained from proactive tests. The fault diagnostics results with the multi-mode data analysis method are compared with those of the single-mode data analysis method. In this section, we elaborate on the two simulated FDD datasets, the evaluation metrics, and the fault diagnostics results.

3.1 Evaluation cases

3.1.1 Simulated FDD datasets of multiple-zone VAV AHU with heating coil

The simulation data used for this part of the evaluation were generated using an HVACSIM+ [36] model of a single duct VAV AHU created from component models in a standard simulation testbed [37-39]. The AHU model includes a chilled water cooling coil and valve, a hot water heating coil and valve, a mixing box with outdoor, recirculation, and exhaust air dampers, and a supply and return fan, as shown in Figure 1. The overall system model includes the AHU and six zones, each equipped with a VAV terminal unit. The model does not account for pressure in the system, instead relying on idealized relationships to determine the flow rate at any point in the system. The AHU operates according to the control sequence presented in Figure 2.

The model was used to simulate the 13 faults listed in Table 7 through modifications of component offset parameters for sensor offset faults, leakage parameters for valve and damper leakage faults, and actuator final control positions for stuck valves and dampers.

Table 7 List of faults of AHU with heating coil chosen to be studied

Fault type	Fault intensity
T_{sa} sensor offset	2 °C, −2 °C
T_{ma} sensor offset	2 °C, −2 °C
T_{oa} sensor offset	2 °C, −2 °C
Stuck recirculation air damper	0%, 50%, 100%
Cooling coil valve (CCV) stuck	Valve stuck 20% open
Heating coil valve (HCV) stuck	Valve stuck 20% open
CCV leaking	Causes the temperature of air flowing across the coil to decrease approximately 2-4°C when the valve is closed
HCV leaking	Causes the temperature of air flowing across the coil to increase

	approximately 2-3°C when the valve is closed

The simulations of each fault were performed using Chicago weather data (any climate could have been used so long as it results in all operational modes for the time periods simulated). Further details of the simulation model are provided in [40]. The data of each of the four operating modes of the AHU were used to test the analysis method described in this paper.

3.1.2 Simulated FDD datasets of multiple-zone VAV AHU without heating coil

The studied system is a single-duct VAV AHU providing cooling to the middle floor of a three-story DOE large office reference building. The conditioned floor space consists of a single interior zone and four perimeter zones. The AHU distributes conditioned air to each zone via one of five VAV boxes. The main components are the same as shown in Figure 1 except there is no hot water heating coil and valve. This AHU only provides cooling and doesn't provide heating. Thus, it only operates under Modes 2, 3, and 4 as illustrated in Section 2.1. Further details of the datasets are provided in [41]. Table 8 lists the fault types, fault intensity and how each fault was imposed in the simulation.

Table 8 List of faults of AHU without heating coil chosen to be studied

Fault type	**Fault intensity**	**Method of fault imposition**
T_{oa} sensor offset	4 °C, −4 °C	Add a bias value to the sensor output
Stuck OA damper	Minimum position 10%, 75%	Override the OA damper position to indicate that the OA damper is stuck
CCV stuck	10% and 75%	Override of the coil valve position to indicate that the valve is stuck

3.2 Evaluation metrics

Fault diagnosis focuses on identifying the CRC of a detected fault. In many studies, the correct diagnosis rate is used to evaluate diagnosis accuracy [9, 20], which is defined as the proportion of cases where the CRC reported by the method matches the true root cause. However, this metric is not suitable for our evaluation as our evaluation focuses on the improvement of diagnosis quality.

In our evaluation, the fault diagnostics results of the new multi-mode method are compared against those of the reference method. When employing the reference method (single-mode fault diagnosis method) as depicted in Table 4, multiple CRCs (including the true root cause) are identified for each satisfied APAR rule. The operators must manually check every possibility to know the true root cause, which is time-consuming and inefficient. Our proposed new method aims to narrow down the range of potential root causes, improving the quality of the diagnosis. In the context of multiple CRCs, the correct diagnosis is defined as one where at least one of the CRCs matches the true root cause, regardless of how many CRCs are returned. This metric does not fully capture the quality of diagnosis and is insufficient for our evaluation. To more effectively quantify the improvement in fault diagnostic resolution and gauge how well the proposed new method narrows down potential root causes, we introduce two metrics, namely the reduced number of CRCs (RN) and the improvement ratio (IR). RN captures the absolute benefits of the multi-mode method, whereas IR reflects a relative or normalized benefit, showing how much the method improves diagnosis quality in comparison to the reference case.

The RN under each evaluation case is calculated as given in Eq. (6).

$$RN = NCRCs_{single-mode} - NCRCs_{multi-mode} \tag{6}$$

Where $NCRCs_{single-mode}$ is the number of CRCs inferred from the reference method and $NCRCs_{multi-mode}$ is the number of CRCs inferred from the multi-mode method.

The IR under each evaluation case is calculated as given in Eq. (7).

$$IR = \frac{(NCRCs_{single-mode} - 1) - (NCRCs_{multi-mode} - 1)}{(NCRCs_{single-mode} - 1)} \text{ when } NCRCs_{single-mode} > 1$$
$$IR = 0 \text{ when } NCRCs_{single-mode} = 1 \tag{7}$$

If the multi-mode method performs better, RN and IR should be positive values. Notedly, a single root cause is the ideal result of a fault diagnostics process. Thus, if the single-mode method identifies more than one CRCs, achieving a single CRC conclusion with the multi-mode method results in a 100% improvement, i.e. IR = 100%. If the single-mode method identifies only one CRC, indicating no potential for improvement, we would report an IR of zero.

3.3 Evaluation Results

3.3.1 Results of multiple-zone VAV AHU with heating coil cases

Both the single-mode method and multi-mode method were applied to the collected data from four operating modes. Table 9 summarizes the fault diagnostics results of the single-mode method under each operating mode, including the rules that were triggered and the CRCs (listed by number based on Table 4) that could have caused those rules to be triggered. Note that if more than one rule is triggered in an operating mode, the list of CRCs in the table is limited to those that are shared by all triggered rules in that mode. "--" means that no rules were satisfied in that mode. The last column summarizes the number of CRCs inferred from the single-mode method. For example, in the case "T_{ma} sensor offset (-2°C)", no rule is activated in Mode 1; rule 7 is satisfied in Mode 2 as the difference between T_{sa} and T_{ma} is greater than the threshold 1.7°C; rule 10 is satisfied in Mode 3 as T_{ma} is less than T_{oa} by 2°C which is larger than the threshold 1.7°C; rule 26 is satisfied in Mode 3 and Mode 4 as T_{ma} is less than the minimum of T_{oa} and T_{ra} in both modes. Recall from Table 4, if use the reference method and only analyzing Mode 4 data, there would be three CRCs presented in the diagnostics results, specifically, T_{ra} sensor error, T_{ma} sensor error, and T_{oa} sensor error (CRC 2, 3,4 in Table 4). Similarly, if only analyzing Mode 2 or 3 data, there would be six or two CRCs. Table 9 shows that when analyzing only the data of one operation mode for the different faults, the diagnostic results include many CRCs. In more than half of the cases, the operator needs to investigate at least six CRCs to determine the ground truth. In the worst cases, the number of CRCs is as high as 11 when analyzing the Mode 4 data in the case "T_{sa} sensor offset (+2°C)" and analyzing the Mode 4 data in the case "CCV Stuck (20% open)".

Table 10 presents the intermediate and final fault diagnostic results of the proposed multi-mode method. The intermediate results include the analysis of triggered APAR rules, the non-triggered APAR rules, and the auxiliary rules. Compared with the results of the single-mode reference method, the proposed multi-mode method results in significantly fewer CRCs. It identifies one CRC in four fault cases, two CRCs in six fault cases, and three to five CRCs in three fault cases. For example, in the case "T_{sa} sensor offset (+2°C)", the shared CRCs identified from triggered rule 7 in Mode 2 and rule 20 in Mode 4 include T_{sa} sensor error, stuck cooling coil valve, leaking heating coil valve, and stuck heating coil valve (CRC 1,6,12,13 in Table 4). Then the analysis of non-triggered APAR rules and the auxiliary rules indicate exclusion rules I, III, IV, V and A1 are satisfied. This means that among the four CRCs identified previously, the stuck cooling coil valve fault and stuck heating coil valve fault (CRC 6 and 13 in Table 4) are not possible and could be removed. As a result, T_{sa} sensor error and leaking heating coil valve are the two CRCs left in the final diagnostic results. In contrast, the analysis of the same data for a single mode of operation presents six or 11 CRCs. The multi-mode method provides a more precise diagnostic result.

Figures 4 and 5 demonstrate how the proposed multi-mode method effectively decreases the number of CRCs in contrast to analyzing data solely for a single mode of operation. Figure 4 lists the reduced number (RN). The bar chart reveals that the multi-mode analysis reduced the number of CRCs by at least three in nine of the 13 fault cases and by at least four in seven of the 13 cases. This represents a potentially significant reduction in the diagnostic effort an operator would need to expend to ultimately find the root cause fault for these cases. Figure 5 lists the improvement ratio (IR). This bar chart shows that an improvement ratio of 80% or greater is achieved in 10 of the 13 fault cases using the multi-mode analysis. Note an improvement ratio of 100% indicates that the root cause fault has been successfully identified as the only CRC. The three faults with the lowest IR values also have the most remaining CRCs following the multi-mode analysis; however, in the case of the "Stuck recirculation air damper (50% open)", the multi-mode analysis did result in a reduction of CRCs by six (i.e., RN = 6).

The sparsity of the results in Figures 4 and 5 is also noteworthy. For a given fault, the improvement achieved with the multi-mode analysis is charted in only one or perhaps two modes. This should not be interpreted as meaning there was no improvement with the multi-mode analysis compared to single-mode analysis for the modes lacking results. Instead, this is indicative that the multi-mode analysis identified one or more CRCs for that fault, whereas the single-mode analysis frequently did not trigger any rules within a particular mode due to masking of the fault symptoms. In another way, in the places where the improvements are not charted, the single mode analysis led you to the conclusion that the AHU is fault free, whereas the multi-mode analysis can reveal the presence of the fault.

Table 9 Fault diagnostics results based on single-mode analysis method (reference method) of the cases “multiple-zone VAV AHU with heating coil”*

Fault	**Triggered APAR Rules & [CRCs]**				**$NCRCs_{single\text{-}mode}$**
	Mode 1 Heating	**Mode 2 Cooling with OA**	**Mode 3 Mech. Cooling with Max OA**	**Mode 4 Mech. Cooling**	
T_{sa} sensor offset (-2°C)	--	7 & [***1***,3,5,6,12,13]	--	--	6
T_{sa} sensor offset (+2°C)	--	7 & [***1***,3,5,6,12,13]	--	20 & [1,6,7,8,9,10,11,12,13, 19,20]	6 or 11
T_{ma} sensor offset (-2°C)	--	7 & [1,***3***,5,6,12,13]	10,26 & [***3***,4]	26 & [2,***3***,4]	6 or 2 or 3
T_{ma} sensor offset (+2°C)	--	7 & [1,***3***,5,6,12,13]	10 & [***3***,4,18,19]	--	4 or 6
T_{oa} sensor offset (-2°C)	--	--	10 & [3,***4***,18,19]	--	4
T_{oa} sensor offset (+2°C)	--	--	10,26 & [3,***4***]	--	2
Stuck recirculation air damper(100% open)	--	--	10 & [3,4,18,***19***]	--	4
Stuck recirculation air damper(0% open)	2 & [2,3,4,***19***]	--	--	18,19,20,25 & [***19***]	1 or 4
Stuck recirculation air damper(50% open)	--	--	--	20 & [1,6,7,8,9,10,11,12,13, ***19***, 20]	11
CCV Stuck (20% open)	1 & [1,3,5,***6***,13, 14,16,17]	7 & [1,3,5,***6***,12,13]	13,14,25 & [1,***6***,7,8, 9, 10, 11,12,13,20]	19,20,25 & [1,***6***,7,8,9,10,11, 12, 13, 19,20]	8 or 6 or 10 or 11
CCV leaking (3% leakage)	--	7 & [1,3,***5***,6,12,13]	--	--	6
HCV stuck (10% open)	4 & [1,5,6,***13***, 14,15,16,17, 20]	7 & [1,3,5,6,12,***13***]	--	--	9 or 6

HCV leaking (3% leakage)	--	7 & [1,3,5,6,***12***,13]	--	--	6

*The ground truth CRC is bold and italicized

Table 10 Fault diagnostics results based on multi-mode analysis method of the cases "multiple-zone VAV AHU with heating coil"*****

Fault	Intermediate diagnostic results			Final diagnostic results	
	Triggered APAR Rules & [Shared CRCs]	**Non-triggered APAR rules & [excluded CRCs]**	**Auxiliary rules & [excluded CRCs]**	**[Final CRCs]**	**$NCRCs_{multi\text{-}mode}$**
T_{sa} sensor offset (-2°C)	7 & [***1***,3,5,6,12,13]	I,III,IV,V &[3,4,6,10,11,13,17]	A2 & [12,13]	[***1***, 5]	2
T_{sa} sensor offset (+2°C)	7,20 & [***1***,6,12,13]	I,III,IV,V &[3,4,6,10,11,13,17]	A1 & [5,6]	[***1***, 12]	2
T_{ma} sensor offset (-2°C)	7,10,26 & [***3***]	I,IV,V & [6,10,11,13,17]	A1 & [5,6]	[***3***]	1
T_{ma} sensor offset (+2°C)	7,10 & [***3***]	I,IV,V & [6,10,11,13,17]	A2 & [12,13]	[***3***]	1
T_{oa} sensor offset (-2°C)	10 & [3,***4***,18,19]	I,II,IV,V & [1, 3, 5, 6, 10, 11,12,13, 17]	- -	[***4***,18,19]	3
T_{oa} sensor offset (+2°C)	10, 26 & [3,***4***]	I,II,IV,V & [1, 3, 5, 6, 10, 11,12,13,17]	- -	[***4***]	1
Stuck recirculation air damper(100% open)	10& [3,4,18,***19***]	I,II,IV,V & [1, 3, 5, 6, 10, 11,12,13,17]	- -	[4, 18, ***19***]	3
Stuck recirculation air damper(0% open)	2,18,19 & [***19***]	I,II,III,IV & [1, 3, 5, 4, 6, 10, 11,12,13, 17]	- -	[***19***]	1
Stuck recirculation air damper(50% open)	20 &[1, 6, 7, 8, 9, 10, 11, 12, 13, ***19***, 20]	I,II,III,IV & [1, 3, 5, 4, 6, 10, 11,12,13, 17]	- -	[7, 8, 9, ***19***, 20]	5
CCV Stuck (20% open)	1, 7, 13, 19 & [1,***6***,13]	I,III & [3,4,13,17]	A2 & [12,13]	[1, ***6***]	2
CCV leaking (3% leakage)	7 &[1,3,***5***,6,12,13]	I,III,IV,V &[3,4,6,10,11,13,17]	A2 & [12,13]	[1, ***5***]	2

HCV stuck (10% open)	4, 7 & [1, 5, 6, ***13***]	III,IV,V &[3,4,6,10,11]	A1 & [5,6]	[1, ***13***]	2
HCV leaking (3% leakage)	7 & [1, 3, 5, 6, ***12***, 13]	I,III,IV,V &[3,4,6,10,11,13,17]	A1 & [5,6]	[1, ***12***]	2

*The ground truth CRC is bold and italicize

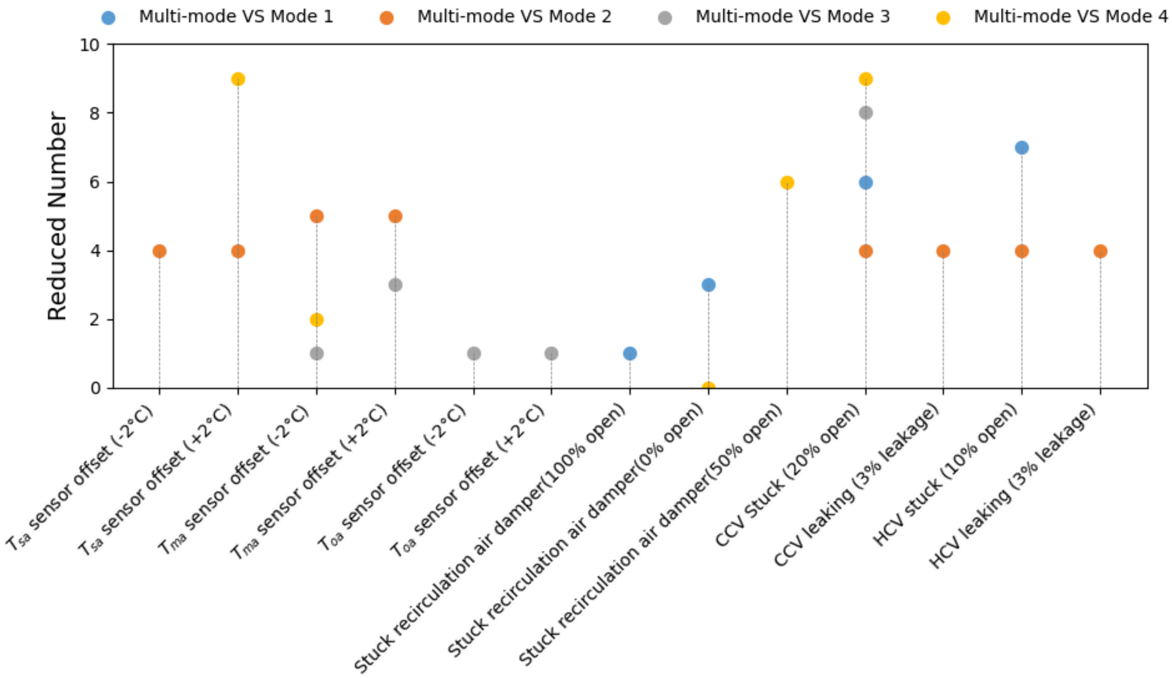

Figure 4 Reduced number of CRCs when implementing multi-mode method in the 13 fault cases of "multiple-zone VAV AHU with heating coil"

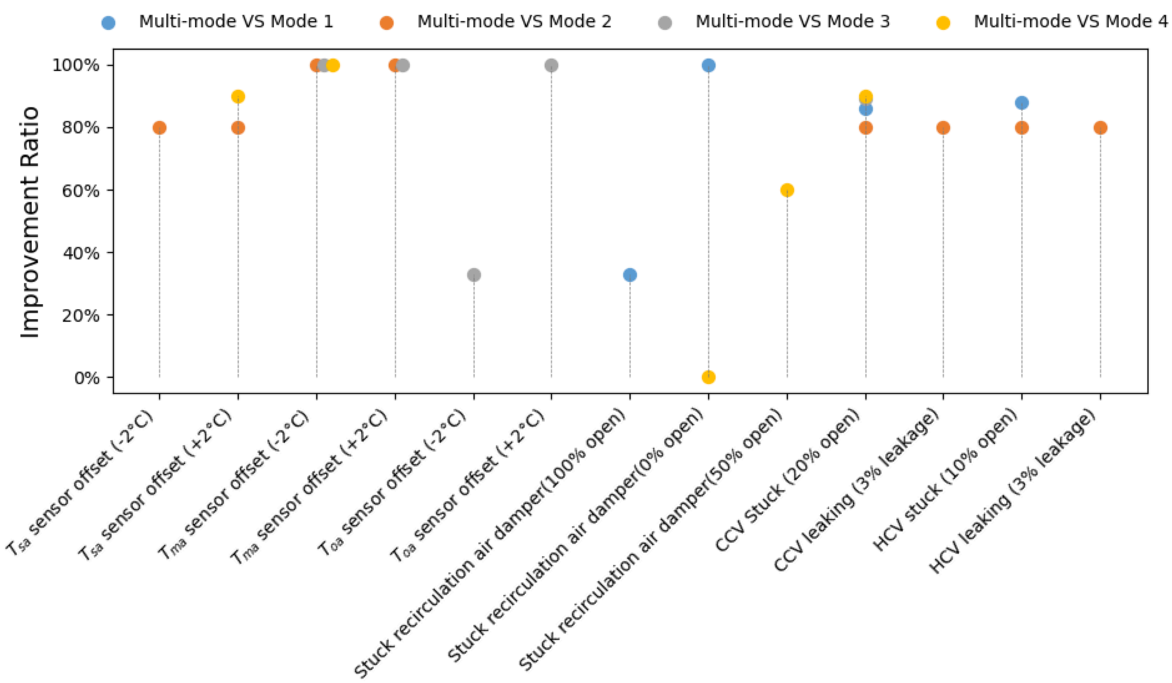

Figure 5 Improvement ratio (IR) when implementing multi-mode method in the 13 fault cases of "multiple-zone VAV AHU with heating coil"

3.3.2 Results of multiple-zone VAV AHU without heating coil

As the multiple-zone VAV AHU without heating coil doesn't provide heating to the space, it only operates under three cooling modes - Modes 2, 3, and 4. Both the single-mode method and multi-mode method were applied to the collected data from three operating modes in the six fault cases as listed in Table 8. It is noted that all the heating coil related CRCs (CRC 12,13,14,15,16,17 in Table 4) are excluded from the analysis, as there is no heating coil in this AHU.

Table 11 and Table 12 summarize the fault diagnostics results of single-mode method and multi-mode method, respectively. Figures 6 and 7 show the capability of the proposed multi-mode method to reduce the number of CRCs compared to the analysis of data for the single mode of operation. As shown in the column "$NCRCs_{single\text{-}mode}$" of Table 11, in five of the six fault cases, the operator needs to examine a minimum of six CRCs to determine the real root cause. For example, in one of the most extreme scenarios, nine CRCs must be inspected when analyzing only the Mode 4 data in the case of "T_{sa} sensor offset (+4°C)". These nine CRCs cover the faults of the T_{sa} sensor, cooling coil, chilled water pumps, mixed box damper, etc. It would be time consuming and labor intensive for the operator to further investigate so many components. In contrast, Table 12 shows that the proposed multi-mode method can lead to a moderate reduced number of CRCs. In the fault case "T_{sa} sensor offset (+4°C)", the multi-mode method listed T_{sa} sensor error as the sole CRC, achieving an IR of 100%. In the fault case "T_{sa} sensor offset (-4°C)", the multi-mode method decreased the number of CRCs from four to two. Figure 6 and

Figure 7 show that the multi-mode method reduced the number of CRCs by at least one and at most eight, and achieved an IR ranging from 14% to 100%.

Table 11 Fault diagnostics results based on single-mode analysis method (reference method) of the cases “multiple-zone VAV AHU without heating coil” *

Fault	Triggered APAR Rules & [CRCs]			$NCRCs_{single\text{-}mode}$
	Mode 2 Cooling with OA	**Mode 3 Mech. Cooling with Max OA**	**Mode 4 Mech. Cooling**	
T_{sa} sensor offset (-4°C)	7 & [***1***,3,5,6]	--	--	4
T_{sa} sensor offset (+4°C)	7 & [***1***,3,5,6]	--	20 & [***1***,6,7,8,9,10,11,19,20]	4 or 9
Stuck OA damper(minimum 10%)	8,10& [4,18,***19***]	10 & [3,4,18,***19***]	--	3 or 4
Stuck OA damper(75%)	--	10 & [3,4,18,***19***]	18&[2,3,4,***19***]	4 or 4
CCV stuck(10%)	--	14 & [1,***6***,7,8,9,10,11,20]	--	8
CCV stuck(75%)	7 & [1,3,5,***6***]	--	19,20&[1,***6***,7,8,9,10,11,20]	4 or 9

*The ground truth CRC is bold and italicized

Table 12 Fault diagnostics results based on multi-mode analysis method of the cases “multiple-zone VAV AHU without heating coil” *

Fault	Intermediate diagnostic results			Final diagnostic results	
	Triggered APAR Rules & [Shared CRCs]	**Non-triggered APAR rules & [excluded CRCs]**	**Auxiliary rules & [excluded CRCs]**	**[Final CRCs]**	$NCRCs_{multi\text{-}mode}$
T_{sa} sensor offset (-4°C)	7 & [***1***,3,5,6]	III,V &[3,4,6,10,11]	--	[***1***, 5]	2
T_{sa} sensor offset (+4°C)	7,20 & [***1***,6]	III,IV,V &[3,4,6,10,11]	A1 & [5,6]	[***1***]	1
Stuck OA damper(minimum 10%)	8,10 & [4,18,***19***]	IV,V & [6,10,11]	--	[4,18,***19***]	3
Stuck OA damper(75%)	10,18 & [3,4,***19***]	I,IV,V & [6,10,11,13,17]	--	[3,4,***19***]	3
CCV stuck(10%)	14 &[1,***6***,7,8,9,10,11,20]	II,III [1,3,4,5,12]	--	[***6***,7,8,9,10,11,20]	7
CCV stuck(75%)	7,19,20 & [1,3,5,***6***]	III & [3,4]	- -	[1,5,***6***]	3

*The ground truth CRC is bold and italicized

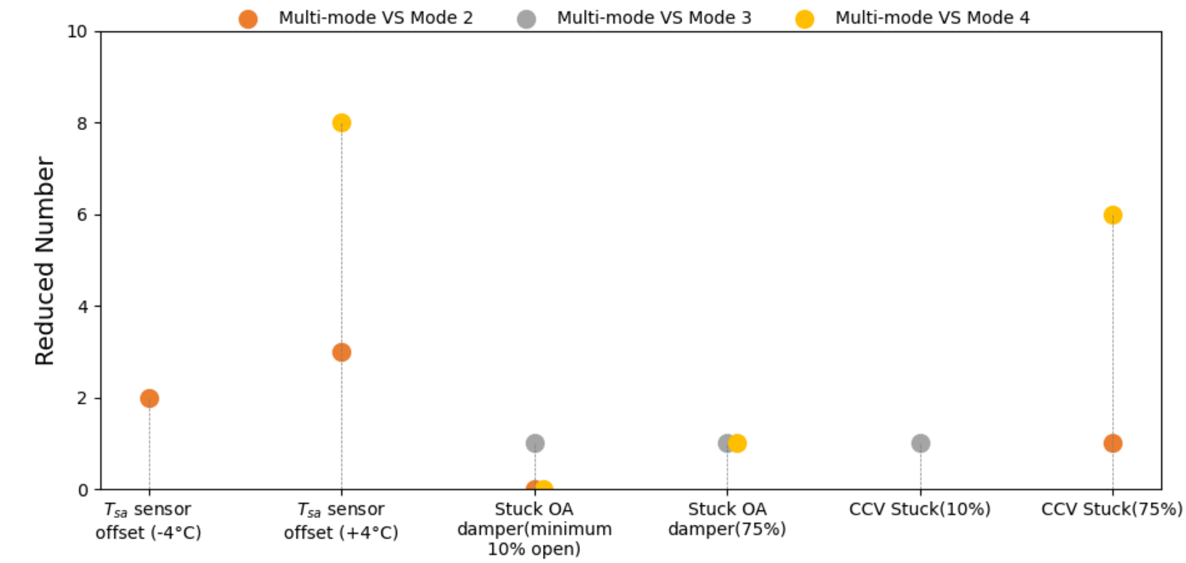

Figure 6 Reduced number of CRCs when implementing multi-mode method in the six fault cases of "multiple-zone VAV AHU without heating coil"

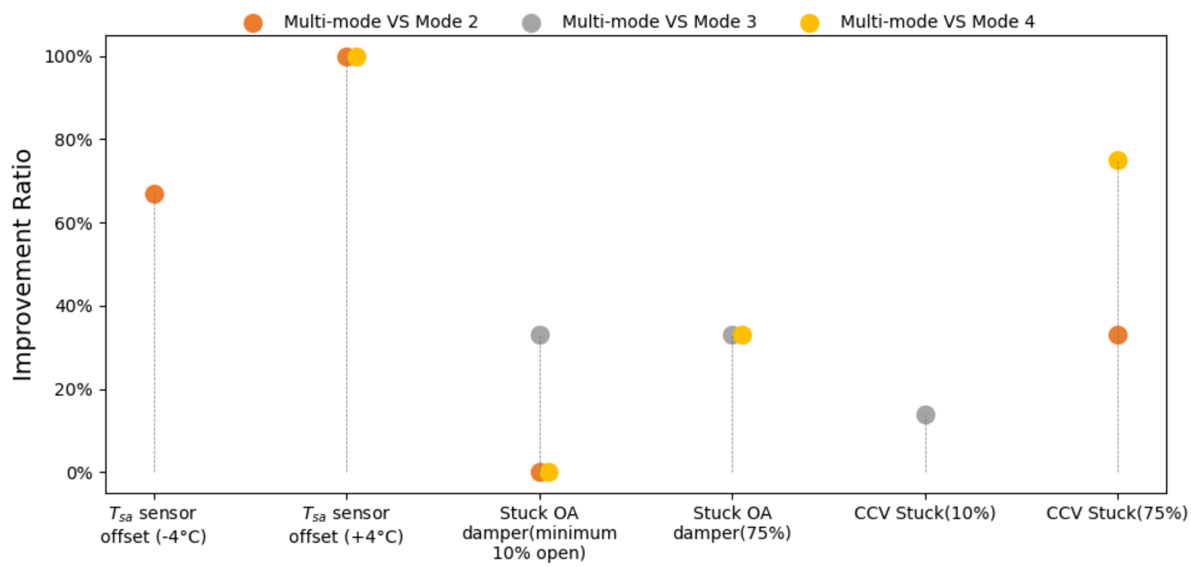

Figure 7 Improvement ratio when implementing multi-mode method in the six fault cases of "multiple-zone VAV AHU without heating coil"

4. Discussion

The proposed rule-based multi-mode data analysis method demonstrated good capability to enhance diagnostic resolution in AHUs, compared with the conventional rule-based single-mode analysis method. For the dataset from the AHU with a heating coil, an improvement ratio of 80% or greater was achieved in 10 of the 13 simulated fault cases. For the AHU without a heating coil, the improvement ratio is 100% in one simulated fault case and ranges from 14% to 75% in the other five cases. The median improvement ratio is 80% in all 19 fault cases. This section provides several points of discussion which navigate the potential improvement of the proposed method in the future.

Firstly, the assessment of the proposed method was conducted with simulated faulty data under all possible operation modes, not with experimental data collected from proactive tests. Although the simulated data used here have many of the same characteristics as data from proactive tests, field testing of the proposed method is needed in future study. A previous study showed that FDD tools have the capability to implement the proactive approach and obtain data for four modes of operation by overriding setpoints [42,43]. As part of our future work, we plan to expand the study to real buildings. We will examine the fault diagnosis resolution improvements, the data collection feasibility, the impact of rule threshold settings and sensor measurement uncertainty, and the effort required for FDD tool integration, to assess the robustness and generalizability of the proposed method.

Secondly, additional proactive functional tests can be developed for further diagnosis. In the fault cases for the AHU with a heating coil, the multi-mode data analysis method has successfully revealed the root cause fault as the only CRC in four fault cases "T_{ma} sensor offset (-2°C)", "T_{ma} sensor offset (+2°C)", "Toa sensor offset (+2°C)", and "Stuck recirculation air damper (0% open)". The method narrowed down the possibility to two CRCs in six cases, three CRCs in two cases, and five CRCs in one case. For the cases where more than one CRCs are identified, additional proactive functional tests can be developed in the future to further screen out the true root cause fault. For example, if "stuck mixing box damper" appeared as one of the remaining CRCs and the return and mixed air temperature sensors are not in the list of CRCs, an open-loop functional test can be conducted to confirm the fault. In this open-loop test, the mixing box dampers can be commanded to 100% recirculation air position (outdoor air damper should be closed) and the heating and coil valves can be commanded to the closed position. If the difference between T_{ra} and T_{ma} is larger than the user-defined temperature threshold ε_t , it can be concluded that a stuck mixing box damper is the correct fault.

Lastly, this study used APAR and auxiliary rules to demonstrate the AHU fault diagnostics enhancement process using the multi-mode analysis method. We believe the generalized procedure presented in the paper can be used and will be effective for other HVAC equipment with multiple modes of operation to facilitate their fault diagnosis. When doing so, we need to collect data from all operation modes and use a rule set with corresponding CRCs. For example, for VAV terminal units, by adjusting the cooling setpoint and heating setpoint respectively, the VAV terminal unit can be forced to operate in heating, cooling, and deadband operational modes respectively. The data recorded under three operational modes can be analyzed with various rules. Then the shared CRCs can be identified from triggered rules and the excluded CRCs can be found from non-triggered rules across three operation modes.

5. Conclusions

Identifying or localizing the root cause of a fault or anomaly is typically more challenging than detecting it, since different root causes can lead to the same fault symptom. However, building facility staff need reliable root causes in order to effectively take action based on FDD software outputs, and therefore to resolve energy and equipment performance problems. Today's commercial FDD tools often fall short of this goal of identifying a root cause fault and instead commonly report behavioral-based faults that offer little diagnostic power. In some instances, the diagnostic results contain multiple distinct CRCs and other cases they offer no insight into possible reasons for the fault. Thus, there is a compelling need to advance the diagnostic capabilities of commercial FDD tools, and the simple and transparent method described in this paper provides one pathway for doing so. That pathway has been opened by two-way communication capabilities between FDD tools and building automation systems, which have been recently validated in real buildings [42,43]. This read and write capability opens the door for FDD tools to perform fault correction, supervisory control, and active testing for improving fault diagnosis.

This study developed a novel active rule-based multi-mode data analysis method to enhance diagnostic resolution by obtaining and combining evidence of both faulty and fault-free behaviors from multiple operational modes. The method is clear and straightforward, enabling its addition to the mainstream rule-based FDD methods which were adopted by most of the commercial FDD tools. In this study, the method was demonstrated using enhanced air handling unit performance assessment rules and validated with the simulated data of two types of AHUs. Two new metrics, namely, reduced number of CRCs and improvement ratio, were proposed to assess the improvement of fault diagnostic resolution. The validation results show that the proposed method achieved a median improvement ratio of 80% in 19 test cases - an improvement ratio of 80% or greater in 10 of the 13 cases of AHU with a heating coil and an improvement ratio ranging from 14% to 100% in the six cases of AHU without a heating coil.

Future work will focus on testing the method under more cases, developing additional proactive functional tests for further diagnosis, and developing proactive tests and auxiliary rules for additional HVAC equipment/systems, building from existing rule sets analogous to APAR.

Nomenclature

Term	Description
u_{hc}	Normalized heating coil valve control signal where 0 = closed and 1 = open [0 - 1]
ε_{hc}	Normalized heating coil valve control signal threshold used in APAR
u_{cc}	Normalized cooling coil valve control signal where 0 = closed and 1 = open [0 - 1]
ε_{cc}	Normalized cooling coil valve control signal threshold used in APAR
u_{dm}	Normalized mixing box damper control signal where 0 = outdoor air damper is fully closed and 1 = outdoor air damper is 100% open [0 - 1]
ε_{dm}	Normalized mixing box damper control signal threshold used in APAR
ε_{t}	Temperature threshold used in APAR and auxiliary rules
ε_{f}	Outdoor airflow fraction threshold used in APAR
ε_{zdat}	A user-selected threshold for the zone discharge air temperature
ε_{zat}	A user-selected threshold for the zone air temperature
ε_{oat}	A user-selected threshold for the outdoor air temperature

CRC_{share}	Shared candidate root causes
T_{zda}	The discharge air temperature from a VAV box
$T_{za,i}$	Zone air temperature of the ith zone [°C]
T_{sa}	Supply air temperature [°C]
$T_{sa,set}$	Supply air temperature setpoint [°C]
T_{ma}	Mixed air temperature [°C]
T_{ra}	Return air temperature [°C]
T_{oa}	Outdoor air temperature [°C]
$T_{oa,ws}$	The ambient air temperature measured by a local weather station
$T_{econ,set}$	Dry bulb economizer setpoint [°C]
ΔT_{rf}	Temperature rise across the return fan used in APAR and auxiliary rules [°C]
ΔT_{sf}	Temperature rise across the supply fan used in APAR [°C]
$\Delta T_{ra,oa,min}$	Minimum temperature difference between the return and outdoor air streams used in APAR [°C]
Q_{oa}/Q_{sa}	Outdoor airflow fraction = (T_{ma} - T_{ra}) / (T_{oa} - T_{ra}) used in APAR
$(Q_{oa}/Q_{sa})_{min}$	Design minimum outdoor air fraction used in APAR
MT_{max}	Threshold for maximum allowable number of mode transitions per hour
N_z	The number of zones considered when determining the median
RN	The reduced number of CRCs
IR	The improvement ratio of CRCs
$NCRCs_{single-mode}$	The number of CRCs inferred from the single-mode method
$NCRCs_{multi-mode}$	Number of CRCs inferred from the multi-mode method

Acronyms

Term	Description
APAR	Air-handling unit Performance Assessment Rules
BN	Bayesian Network
CCV	Cooling Coil Valve
CRC(s)	Candidate Root Cause(s)
FDD	Fault Detection and Diagnosis
HCV	Heating Coil Valve
HVAC	Heating, Ventilation, and Air Conditioning
PCA	Principal Components Analysis
OA	Outdoor Air
VAV	Variable-Air-Volume

Declaration of competing interest

The authors declare that they have no known competing financial interests or personal relationships that could have appeared to influence the work reported in this paper.

Acknowledgements

This work was supported by the Assistant Secretary for Energy Efficiency and Renewable Energy, Building Technologies Office, of the U.S. Department of Energy under Contract No. DE-AC02-05CH11231. The authors wish to acknowledge Cecilia Johnson, Amir Roth, and Michael Blunschi for their guidance and support of the research.

References

[1] R. Jagpal, Computer aided evaluation of HVAC system performance: Technical synthesis report, International Energy Agency (2006).

[2] Z. Chen, Z. O'Neill, J. Wen, O. Pradhan, T. Yang, X. Lu, G. Lin, S. Miyata, S. Lee, C. Shen, R. Chiosa, M.S. Piscitelli, A. Capozzoli, F. Hengel, A. Kührer, M. Pritoni, W. Liu, J. Clauß, Y. Chen, T. Herr, A review of data-driven fault detection and diagnostics for building HVAC systems, Applied Energy 339 (2023) 121030. https://doi.org/10.1016/j.apenergy.2023.121030.

[3] J. Chen, L. Zhang, Y. Li, Y. Shi, X. Gao, Y. Hu, A review of computing-based automated fault detection and diagnosis of heating, ventilation and air conditioning systems, Renewable and Sustainable Energy Reviews 161 (2022) 112395. https://doi.org/10.1016/j.rser.2022.112395.

[4] Y. Yu, D. Woradechjumroen, D. Yu, A review of fault detection and diagnosis methodologies on air-handling units, Energy and Buildings 82 (2014) 550–562. https://doi.org/10.1016/j.enbuild.2014.06.042.

[5] S. Katipamula, M.R. Brambley, Review Article: Methods for fault detection, diagnostics, and prognostics for building systems—a review, part I, HVAC&R Research 11 (2005) 3–25. https://doi.org/10.1080/10789669.2005.10391123.

[6] G. Lin, H. Kramer, V. Nibler, E. Crowe, J. Granderson, Building analytics tool deployment at scale: benefits, costs, and deployment practices, Energies 15 (2022). https://doi.org/10.3390/en15134858.
[7] S. Frank, G. Lin, X. Jin, R. Singla, A. Farthing, J. Granderson, A performance evaluation framework for building fault detection and diagnosis algorithms, Energy and Buildings 192 (2019) 84–92. https://doi.org/10.1016/j.enbuild.2019.03.024.
[8] E. Crowe, Y. Chen, H. Reeve, D. Yuill, A. Ebrahimifakhar, Y. Chen, L. Troup, A. Smith, J. Granderson, Empirical analysis of the prevalence of HVAC faults in commercial buildings, Science and Technology for the Built Environment 29 (2023) 1027–1038. https://doi.org/10.1080/23744731.2023.2263324.
[9] G. Lin, H. Kramer, J. Granderson, Building fault detection and diagnostics: Achieved savings, and methods to evaluate algorithm performance, Building and Environment 168 (2020) 106505. https://doi.org/10.1016/j.buildenv.2019.106505.
[10] K. Bruton, P. Raftery, B. Kennedy, M.M. Keane, D.T.J. O'Sullivan, Review of automated fault detection and diagnostic tools in air handling units, Energy Efficiency 7 (2014) 335–351. https://doi.org/10.1007/s12053-013-9238-2.
[11] Z. Shi, W. O'Brien, Development and implementation of automated fault detection and diagnostics for building systems: A review, Automation in Construction 104 (2019) 215–229. https://doi.org/10.1016/j.autcon.2019.04.002.
[12] Y. Zhao, T. Li, X. Zhang, C. Zhang, Artificial intelligence-based fault detection and diagnosis methods for building energy systems: Advantages, challenges and the future, Renewable and Sustainable Energy Reviews 109 (2019) 85–101. https://doi.org/10.1016/j.rser.2019.04.021.
[13] A. Ebrahimifakhar, A. Kabirikopaei, D. Yuill, Data-driven fault detection and diagnosis for packaged rooftop units using statistical machine learning classification methods, Energy and Buildings 225 (2020) 110318. https://doi.org/10.1016/j.enbuild.2020.110318.
[14] A. Montazeri, S.M. Kargar, Fault detection and diagnosis in air handling using data-driven methods, Journal of Building Engineering 31 (2020) 101388. https://doi.org/10.1016/j.jobe.2020.101388.
[15] K. Yan, J. Huang, W. Shen, Z. Ji, Unsupervised learning for fault detection and diagnosis of air handling units, Energy and Buildings 210 (2020) 109689. https://doi.org/10.1016/j.enbuild.2019.109689.
[16] R. Wu, Y. Ren, M. Tan, L. Nie, Fault diagnosis of HVAC system with imbalanced data using multi-scale convolution composite neural network, Building Simulation 17 (2024) 371–386. https://doi.org/10.1007/s12273-023-1086-1.
[17] P. Li, Z. Liu, B. Anduv, X. Zhu, X. Jin, Z. Du, Diagnosis for multiple faults of chiller using ELM-KNN model enhanced by multi-label learning and specific feature combinations. Building and Environment (2022) 214 108904. https://doi.org/10.1016/j. buildenv.2022.108904.
[18] K.-P. Lee, B.-H. Wu, S.-L. Peng, Deep-learning-based fault detection and diagnosis of air-handling units, Building and Environment 157 (2019) 24–33. https://doi.org/10.1016/j.buildenv.2019.04.029.
[19] M. Liu, L. Zhang, J. Chen, W.A. Chen, Z. Yang, L.J. Lo, J. Wen, Z. O'Neill, Large language models for building energy applications: Opportunities and challenges. Building Simulation (2025). https://doi.org/10.1007/s12273-025-1235-9
[20] J. Zhang, C. Zhang, J. Lu, Y. Zhao, Domain-specific large language models for fault diagnosis of heating, ventilation, and air conditioning systems by labeled-data-supervised fine-tuning. Applied Energy 377(2025) 124378. https://doi.org/10.1016/j.apenergy.2024.124378
[21] J. Granderson, G. Lin, R. Singla, E. Mayhorn, P. Ehrlich, D. Vrabie, S. Frank, Commercial Fault Detection and Diagnostics Tools: What They Offer, How They Differ, and What's Still Needed, (2018). https://doi.org/10.20357/B7V88H.

[22] Y. Zhao, J. Wen, F. Xiao, X. Yang, S. Wang, Diagnostic Bayesian networks for diagnosing air handling units faults – part I: Faults in dampers, fans, filters and sensors, Applied Thermal Engineering 111 (2017) 1272–1286. https://doi.org/10.1016/j.applthermaleng.2015.09.121.
[23] F. Xiao, Y. Zhao, J. Wen, S. Wang, Bayesian network based FDD strategy for variable air volume terminals, Automation in Construction 41 (2014) 106–118. https://doi.org/10.1016/j.autcon.2013.10.019.
[24] Y. Zhao, F. Xiao, S. Wang, An intelligent chiller fault detection and diagnosis methodology using Bayesian belief network, Energy and Buildings 57 (2013) 278–288. https://doi.org/10.1016/j.enbuild.2012.11.007.
[25] Z. Wang, Z. Wang, S. He, X. Gu, Z.F. Yan, Fault detection and diagnosis of chillers using Bayesian network merged distance rejection and multi-source non-sensor information, Applied Energy 188 (2017) 200–214. https://doi.org/10.1016/j.apenergy.2016.11.130.
[26] Z. Liu, Y. Liu, D. Zhang, B. Cai, C. Zheng, Fault diagnosis for a solar assisted heat pump system under incomplete data and expert knowledge, Energy 87 (2015) 41–48. https://doi.org/10.1016/j.energy.2015.04.090.
[27] Y. Chen, J. Wen, O. Pradhan, L.J. Lo, T. Wu, Using discrete Bayesian networks for diagnosing and isolating cross-level faults in HVAC systems, Applied Energy 327 (2022) 120050. https://doi.org/10.1016/j.apenergy.2022.120050.
[28] T. Gao, S. Marié, P. Béguery, S. Thebault, S. Lecoeuche, Integrated building fault detection and diagnosis using data modeling and Bayesian networks, Energy and Buildings 306 (2024) 113889. https://doi.org/10.1016/j.enbuild.2024.113889.
[29] J. House, H. Vaezi-Nejad, An expert rule set for fault detection in air-handling units, ASHRAE Transactions. 107 (2001) (1):858-871.
[30] J. Schein, S.T. Bushby, N.S. Castro, J.M. House, A rule-based fault detection method for air handling units, Energy and Buildings 38 (2006) 1485–1492. https://doi.org/10.1016/j.enbuild.2006.04.014.
[31] N. Milesi-Ferretti, M. Galler, S. Bushby, Evaluating the Initial Field Performance of HVAC-Cx for Air Handling Units. National Institute of Standards and Technology Technical Note 1924 (2016). http://dx.doi.org/10.6028/NIST.TN.1924
[32] O. Nehasil, L. Dobiášová, V. Mazanec, J. Široký, Versatile AHU fault detection – Design, field validation and practical application. Energy and Buildings 237(2021), 110781. https://doi.org/10.1016/j.enbuild.2021.110781
[33] H. Hosamo, P. Svennevig, K. Svidt, D. Han, H. Nielsen, A Digital Twin predictive maintenance framework of air handling units based on automatic fault detection and diagnostics. Energy and Buildings (2022) 261, 111988. https://doi.org/10.1016/j.enbuild.2022.111988
[34] S. Li, J. Wen. Development and Validation of a Dynamic Air handling Unit Model, Part I. ASHRAE ASHRAE Transactions 116(2010):45.
[35] S. Li, J. Wen, X. Zhou, CJ. Klaassen CJ. Development and Validation of a Dynamic Air Handling Unit Model, Part 2. ASHRAE Transactions 116(2010):57–73.
[36] C. Park, An overview of HVACSIM^+, A Dynamic Building/HVAC/Control System Simulation Program, in: Proc. 1st Annual Building Energy Simulation Conference, Seattle, WA, USA, 1985. https://cir.nii.ac.jp/crid/1570854174512026752 (accessed November 22, 2024).
[37] L.K. Norford, P. Haves, A standard simulation testbed for the evaluation of control algorithms and strategies, Final Report of ASRAE 825-RP (1997).
[38] P. Haves, L.K. Norford, M. DeSimone, A standard simulation test bed for the evaluation of control algorithms and strategies, ASHRAE Transactions 104 (1998) 460. Retrieved from https://www.proquest.com/scholarly-journals/standard-simulation-test-bed-evaluation-control/docview/192541415/se-2.

[39] M. DeSimone, A standard simulation testbed for the evaluation of control algorithms & strategies related to variable air volume HVAC systems, PhD Thesis, Massachusetts Institute of Technology, 1995. https://dspace.mit.edu/handle/1721.1/37035 (accessed November 22, 2024).
[40] J.E. Seem, J.M. House, Integrated Control and Fault Detection of Air-Handling Units, HVAC&R Research 15 (2009) 25–55. https://doi.org/10.1080/10789669.2009.10390824.
[41] J. Granderson, G. Lin, Y. Chen, A. Casillas, J. Wen, Z. Chen, P. Im, S. Huang, J. Ling, A labeled dataset for building HVAC systems operating in faulted and fault-free states, Scientific Data 10 (2023) 342. https://doi.org/10.1038/s41597-023-02197-w.
[42] G. Lin, M. Pritoni, Y. Chen, J. Granderson, Development and implementation of fault-correction algorithms in fault detection and diagnostics tools, Energies 13 (2020). https://doi.org/10.3390/en13102598.
[43] M. Pritoni, G. Lin, Y. Chen, R. Vitti, C. Weyandt, J. Granderson, From fault-detection to automated fault correction: A field study, Building and Environment 214 (2022) 108900. https://doi.org/10.1016/j.buildenv.2022.108900.